SIAM J. NUMER. ANAL.
Vol. 47, No. 1, pp. 1–19

MIXED FINITE ELEMENT FORMULATION AND ERROR ESTIMATES BASED ON PROPER ORTHOGONAL DECOMPOSITION FOR THE NONSTATIONARY NAVIER–STOKES EQUATIONS*

ZHENDONG LUO†, JING CHEN‡, I. M. NAVON§, AND XIAOZHONG YANG†

Abstract. In this paper, proper orthogonal decomposition (POD) is used for model reduction of mixed finite element (MFE) for the nonstationary Navier–Stokes equations and error estimates between a reference solution and the POD solution of reduced MFE formulation are derived. The basic idea of this reduction technique is that ensembles of data are first compiled from transient solutions computed equation system derived with the usual MFE method for the nonstationary Navier–Stokes equations or from physics system trajectories by drawing samples of experiments and interpolation (or data assimilation), and then the basis functions of the usual MFE method are substituted with the POD basis functions reconstructed by the elements of the ensemble to derive the POD-reduced MFE formulation for the nonstationary Navier–Stokes equations. It is shown by considering numerical simulation results obtained for the illustrating example of cavity flows that the error between POD solution of reduced MFE formulation and the reference solution is consistent with theoretical results. Moreover, it is also shown that this result validates the feasibility and efficiency of the POD method.

Key words. mixed finite element method, proper orthogonal decomposition, the nonstationary Navier–Stokes equations, error estimate

AMS subject classifications. 65N30, 35Q10

DOI. 10.1137/070689498

1. Introduction.

The mixed finite element (MFE) method is one of the important approaches for solving systems of partial differential equations, for example, the nonstationary Navier–Stokes equations (see [1], [2], or [3]). However, the computational model for the fully discrete system of MFE solutions of the nonstationary Navier–Stokes equations yields very large systems that are computationally intensive. Thus, an important problem is how to simplify the computational load and save time-consuming calculations and resource demands in the actual computational process in a way that guarantees a sufficiently accurate and efficient numerical solution. Proper orthogonal decomposition (POD), also known as Karhunen–Loève expansions in signal analysis and pattern recognition (see [4]), or principal component analysis in statistics (see [5]), or the method of empirical orthogonal functions in geophysical fluid dynamics (see [6], [7]) or meteorology (see [8]), is a technique offering adequate approximation for representing fluid flow with reduced number of degrees of freedom, i.e., with lower dimensional models (see [9]), so as to alleviate the computational load

*Received by the editors April 25, 2007; accepted for publication (in revised form) May 19, 2008; published electronically October 24, 2008.
http://www.siam.org/journals/sinum/47-1/68949.html
†School of Mathematics and Physics, North China Electric Power University, Beijing 102206, China (zhdluo@163.com). This work was supported in part by the National Science Foundation of China (NSF10871022 and 10771065).
‡Corresponding author. College of Science, China Agricultural University, Beijing 100083, China (jing_quchen@163.com). This author was supported in part by the National Science Foundation of China (NSF10871022 and 10771213).
§Department of Scientific Computing, Florida State University, Dirac Sci. Lib. Bldg., #483, Tallahassee, FL 32306-4120 (navon@scs.fsu.edu). This author was supported in part by NASA MAP grant Modeling, Analysis and Prediction Program (NNG06GC67G).

and provide CPU and memory requirements savings, and has found widespread applications in problems related to the approximation of large-scale models. Although the basic properties of the POD method are well established and studies have been conducted to evaluate the suitability of this technique for various fluid flows (see [10]–[12]), its applicability and limitations for reduced MFE formulation for the nonstationary Navier–Stokes equations are not well documented.

The POD method mainly provides a useful tool for efficiently approximating a large amount of data. The method essentially provides an orthogonal basis for representing the given data in a certain least squares optimal sense; that is, it provides a way to find optimal lower dimensional approximations of the given data. In addition to being optimal in a least squares sense, POD has the property that it uses a modal decomposition that is completely data dependent and does not assume any prior knowledge of the process used to generate the data. This property is advantageous in situations where a priori knowledge of the underlying process is insufficient to warrant a certain choice of basis. Combined with the Galerkin projection procedure, POD provides a powerful method for generating lower dimensional models of dynamical systems that have a very large or even infinite dimensional phase space. In many cases, the behavior of a dynamic system is governed by characteristics or related structures, even though the ensemble is formed by a large number of different instantaneous solutions. POD method can capture these temporal and spatial structures by applying a statistical analysis to the ensemble of data. In fluid dynamics, Lumley first employed the POD technique to capture the large eddy coherent structures in a turbulent boundary layer (see [13]); this technique was further extended in [14], where a link between the turbulent structure and dynamics of a chaotic system was investigated. In Holmes, Lumley, and Berkooz [9], the overall properties of POD are reviewed and extended to widen the applicability of the method. The method of snapshots was introduced by Sirovich [15], and is widely used in applications to reduce the order of POD eigenvalue problem. Examples of these are optimal flow control problems [16]–[18] and turbulence [9, 13, 14, 19, 20]. In many applications of POD, the method is used to generate basis functions for a reduced order model, which can simplify and provide quicker assessment of the major features of the fluid dynamics for the purpose of flow control as demonstrated by Ko et al. [18] or design optimization as shown by Ly and Tran [17]. This application is used in a variety of other physical applications, such as in [17], which demonstrates an effective use of POD for a chemical vapor deposition reactor. Some reduced order finite difference models and MFE formulations and error estimates based on POD for the upper tropical Pacific Ocean model (see [21]–[25]), as well as a finite difference scheme based on POD for the nonstationary Navier–Stokes equations (see [26]), have been derived. However, to the best of our knowledge, there are no published results addressing the use of POD to reduce the MFE formulation of the nonlinear nonstationary Navier–Stokes equations and provide estimates of the error between reference solution and the POD-reduced MFE solution.

In this paper, POD is used to reduce the MFE formulation for the nonstationary Navier–Stokes equations and to derive error estimates between reference solution and the POD-reduced MFE solution. It is shown by considering the results obtained for numerical simulations of cavity flows that the error between POD solution of reduced MFE formulation and reference solution is consistent with theoretically derived results. Moreover, it is also shown that this validates the feasibility and efficiency of the POD method. Though Kunisch and Volkwein have presented some Galerkin POD methods for parabolic problems and a general equation in fluid dynamics in [27], [28], our method is different from their approaches, whose methods consist of Galerkin projection where the original variables are substituted for a linear combination of POD basis and the error estimates of the velocity field therein are only derived, their POD basis being generated with the solution of the physical system at all time instances. In particular, the velocity field is only approximated in [28], while both velocity and pressure fields are simultaneously approximated in our present method. While the singular value decomposition approach combined with POD methodology is used to treat the Burgers equation in [29] and the cavity flow problem in [12], the error estimates have not completely been derived, in particular, a reduced formulation of MFE for the nonstationary Navier–Stokes has not yet been derived up to now. Therefore, our method improves upon existing methods since our POD basis is generated with the solution of the physical system only at time instances which are both useful and of interest for us.

2. MFE approximation for the nonstationary Navier–Stokes equations and snapshots generate. Let $\Omega \subset R^2$ be a bounded, connected, and polygonal domain. Consider the following nonstationary Navier–Stokes equations.

Problem (I) Find $\boldsymbol{u} = (u_1, u_2)$, p such that, for $T > 0$,

$$\begin{cases} \boldsymbol{u}_t - \nu\triangle\boldsymbol{u} + (\boldsymbol{u}\cdot\nabla)\boldsymbol{u} + \nabla p = \boldsymbol{f} & \text{in } \Omega\times(0,T), \\ \text{div}\boldsymbol{u} = 0 & \text{in } \Omega\times(0,T), \\ \boldsymbol{u}(x,y,t) = \boldsymbol{\varphi}(x,y,t) & \text{on } \partial\Omega\times(0,T), \\ \boldsymbol{u}(x,y,0) = \boldsymbol{\varphi}(x,y,0) & \text{in } \Omega, \end{cases} \tag{2.1}$$

where $\boldsymbol{u}$ represents the velocity vector, p the pressure, ν the constant inverse Reynolds number, $\boldsymbol{f} = (f_1, f_2)$ the given body force, and $\boldsymbol{\varphi}(x,y,t)$ the given vector function. For the sake of convenience, without lost generality, we may as well suppose that $\boldsymbol{\varphi}(x,y,t)$ is a zero vector in the following theoretical analysis.

The Sobolev spaces used in this context are standard (see [30]). For example, for a bounded domain Ω, we denote by $H^m(\Omega)$ $(m \ge 0)$ and $L^2(\Omega) = H^0(\Omega)$ the usual Sobolev spaces equipped with the seminorm and the norm, respectively,

$$|v|_{m,\Omega} = \left\{\sum_{|\boldsymbol{\alpha}|=m}\int_\Omega |D^{\boldsymbol{\alpha}}v|^2\mathrm{d}x\mathrm{d}y\right\}^{1/2} \text{ and } \|v\|_{m,\Omega} = \left\{\sum_{i=0}^m |v|_{i,\Omega}^2\right\}^{1/2} \quad \forall v \in H^m(\Omega),$$

where $\boldsymbol{\alpha} = (\alpha_1, \alpha_2)$, α_1 and α_2 are two nonnegative integers, and $|\boldsymbol{\alpha}| = \alpha_1 + \alpha_2$. Especially, the subspace $H_0^1(\Omega)$ of $H^1(\Omega)$ is denoted by

$$H_0^1(\Omega) = \left\{v \in H^1(\Omega); u|_{\partial\Omega} = 0\right\}.$$

Note that $\|\cdot\|_1$ is equivalent to $|\cdot|_1$ in $H_0^1(\Omega)$. Let $L_0^2(\Omega) = \left\{q \in L^2(\Omega); \int_\Omega q\mathrm{d}x\mathrm{d}y = 0\right\}$, which is a subspace of $L^2(\Omega)$. It is necessary to introduce the Sobolev spaces dependent on time t in order to discuss the generalized solution for Problem (I). Let Φ be a Hilbert space. For all $T > 0$ and integer $n \ge 0$, for $t \in [0,\ T]$, define

$$H^n(0,T;\Phi) = \left\{v(t) \in \Phi;\ \int_0^T \sum_{i=0}^n \left\|\frac{\mathrm{d}^i}{\mathrm{d}t^i}v(t)\right\|_\Phi^2 \mathrm{d}t < \infty\right\},$$

which is endowed with the norm

$$\|v\|_{H^n(\Phi)} = \left[\sum_{i=0}^n \int_0^T \left\|\frac{\mathrm{d}^i}{\mathrm{d}t^i}v(t)\right\|_\Phi^2 \mathrm{d}t\right]^{\frac{1}{2}} \quad \text{for } v \in H^n(\Phi),$$

where $\|\cdot\|_\Phi$ is the norm of space Φ. Especially, if $n = 0$,

$$\|v\|_{L^2(\Phi)} = \left(\int_0^T \|v(t)\|_\Phi^2 \mathrm{d}t\right)^{\frac{1}{2}}.$$

And define

$$L^\infty(0,T;\Phi) = \left\{v(t) \in \Phi;\ \operatorname*{ess\,sup}_{0\le t\le T} \|v(t)\|_\Phi < \infty\right\},$$

which is endowed with the norm

$$\|v\|_{L^\infty(\Phi)} = \operatorname*{ess\,sup}_{0\le t\le T} \|v(t)\|_\Phi.$$

The variational formulation for Problem (I) is written as:

Problem (II) Find $(\boldsymbol{u}, p) \in H^1(0,T;X) \times L^2(0,T;M)$ such that, for all $t \in (0,T)$,

$$\left\{\begin{array}{l} (\boldsymbol{u}_t, \boldsymbol{v}) + a(\boldsymbol{u}, \boldsymbol{v}) + a_1(\boldsymbol{u}, \boldsymbol{u}, \boldsymbol{v}) - b(p, \boldsymbol{v}) = (\boldsymbol{f}, \boldsymbol{v}) \quad \forall \boldsymbol{v} \in X, \\ b(q, \boldsymbol{u}) = 0 \qquad \forall q \in M, \\ \boldsymbol{u}(x,0) = \boldsymbol{0} \quad \text{in } \Omega, \end{array}\right. \tag{2.2}$$

where $X = H_0^1(\Omega)^2$, $M = L_0^2(\Omega)$, $a(\boldsymbol{u}, \boldsymbol{v}) = \nu \int_\Omega \nabla \boldsymbol{u} \cdot \nabla \boldsymbol{v} \mathrm{d}x\mathrm{d}y$, $a_1(\boldsymbol{u}, \boldsymbol{v}, \boldsymbol{w}) = \frac{1}{2}\int_\Omega \sum_{i,j=1}^2 [u_i \frac{\partial v_j}{\partial x_i} w_j - u_i \frac{\partial w_j}{\partial x_i} v_j] \mathrm{d}x\mathrm{d}y$ $(\boldsymbol{u}, \boldsymbol{v}, \boldsymbol{w} \in X)$, and $b(q, \boldsymbol{v}) = \int_\Omega q \operatorname{div} \boldsymbol{v} \mathrm{d}x\mathrm{d}y$.

Throughout the paper, C indicates a positive constant which is possibly different at different occurrences, being independent of the spatial and temporal mesh sizes, but may depend on Ω, the Reynolds number, and other parameters introduced in this paper.

The following property for trilinear form $a_1(\cdot,\cdot,\cdot)$ is often used (see [1], [2], or [3]).

$$a_1(\boldsymbol{u}, \boldsymbol{v}, \boldsymbol{w}) = -a_1(\boldsymbol{u}, \boldsymbol{w}, \boldsymbol{v}), \quad a_1(\boldsymbol{u}, \boldsymbol{v}, \boldsymbol{v}) = 0 \quad \forall \boldsymbol{u}, \boldsymbol{v}, \boldsymbol{w} \in X. \tag{2.3}$$

The bilinear forms $a(\cdot,\cdot)$ and $b(\cdot,\cdot)$ have the following properties:

$$a(\boldsymbol{v}, \boldsymbol{v}) \ge \nu |\boldsymbol{v}|_1^2 \quad \forall \boldsymbol{v} \in H_0^1(\Omega)^2, \tag{2.4}$$

$$|a(\boldsymbol{u}, \boldsymbol{v})| \le \nu |u|_1 |\boldsymbol{v}|_1 \quad \forall \boldsymbol{u},\ \boldsymbol{v} \in H_0^1(\Omega)^2, \tag{2.5}$$

and

$$\sup_{\boldsymbol{v} \in H_0^1(\Omega)^2} \frac{b(q, \boldsymbol{v})}{|\boldsymbol{v}|_1} \ge \beta \|q\|_0 \quad \forall q \in L_0^2(\Omega), \tag{2.6}$$

where β is a positive constant. Define

$$N = \sup_{\boldsymbol{u}, \boldsymbol{v}, \boldsymbol{w} \in X} \frac{a_1(\boldsymbol{u}, \boldsymbol{v}, \boldsymbol{w})}{|\boldsymbol{u}|_1 |\boldsymbol{v}|_1 |\boldsymbol{w}|_1}; \quad \|\boldsymbol{f}\|_{-1} = \sup_{\boldsymbol{v} \in X} \frac{(\boldsymbol{f}, \boldsymbol{v})}{|\boldsymbol{v}|_1}. \tag{2.7}$$

The following result is classical (see [1], [2], or [3]).

THEOREM 2.1. *If* $\boldsymbol{f} \in L^2(0,T;H^{-1}(\Omega)^2)$, *then Problem* (II) *has at least a solution which, in addition, is unique provided that* $\nu^{-2} N \|\boldsymbol{f}\|_{L^2(H^{-1})} < 1$, *and there is the following prior estimate:*

$$\|\nabla \boldsymbol{u}\|_{L^2(L^2)} \le \nu^{-1} \|\boldsymbol{f}\|_{L^2(H^{-1})} \equiv R, \quad \|\boldsymbol{u}\|_0 \le \nu^{-1/2} \|\boldsymbol{f}\|_{L^2(H^{-1})} = R\nu^{-1/2}.$$

Let $\{\Im_h\}$ be a uniformly regular family of triangulation of $\bar{\Omega}$ (see [31], [32], or [33]), indexed by a parameter $h = \max_{K\in\Im_h}\{h_K;\ h_K = \text{diam}(K)\}$; i.e., there exists a constant C, independent of h, such that $h \le Ch_K\ \forall K \in \Im_h$.

We introduce the following finite element spaces X_h and M_h of X and M, respectively. Let $X_h \subset X$ (which is at least the piecewise polynomial vector space of mth degree, where $m > 0$ is integer) and $M_h \subset M$ (which is the piecewise polynomial space of $(m-1)$th degree). Write $\hat{X}_h = X_h \times M_h$.

We assume that (X_h, M_h) satisfies the following approximate properties: $\forall v \in H^{m+1}(\Omega)^2 \cap X$ and $\forall q \in M \cap H^m(\Omega)$,

$$\inf_{\boldsymbol{v}_h\in X_h} \|\nabla(\boldsymbol{v}-\boldsymbol{v}_h)\|_0 \le Ch^m|\boldsymbol{v}|_{m+1}, \quad \inf_{q_h\in M_h} \|q-q_h\|_0 \le Ch^m|q|_m, \tag{2.8}$$

together the so-called discrete LBB condition, i.e.,

$$\sup_{\boldsymbol{v}_h\in X_h} \frac{b(q_h,\boldsymbol{v}_h)}{\|\nabla\boldsymbol{v}_h\|_0} \ge \beta\|q_h\|_0 \quad \forall q_h \in M_h, \tag{2.9}$$

where β is a positive constant independent of h.

There are many spaces X_h and M_h satisfying the discrete LBB conditions (see [33]). Here, we provide some examples as follows.

Example 2.1. The first-order finite element space $X_h \times M_h$ can be taken as Bernardi–Fortin–Raugel's element (see [33]), i.e.,

$$\begin{aligned} X_h &= \left\{\boldsymbol{v}_h \in X \cap C^0(\bar{\Omega})^2;\ \boldsymbol{v}_{h|K} \in P_K \quad \forall K \in \Im_h\right\}, \\ M_h &= \left\{\varphi_h \in M;\ \varphi_{h|K} \in P_0(K) \quad \forall K \in \Im_h\right\}, \end{aligned} \tag{2.10}$$

where $P_K = P_1(K)^2 \oplus \text{span}\{\boldsymbol{n}_i \prod_{j=1,j\ne i}^3 \lambda_{Kj},\ i = 1,2,3\}$, $\boldsymbol{n}_i$ are the unit normal vector to side F_i opposite the vertex A_i of triangle K, λ_{Ki}'s are the barycenter coordinates corresponding to the vertex A_i $(i = 1,2,3)$ on K (see [31], [32]), and $P_m(K)$ is the space of piecewise polynomials of degree m on K.

Example 2.2. The first-order finite element space $X_h \times M_h$ can also be taken as Mini's element, i.e.,

$$\begin{aligned} X_h &= \left\{\boldsymbol{v}_h \in X \cap C^0(\Omega)^2;\ \boldsymbol{v}_h|_K \in P_K \quad \forall K \in \Im_h\right\}, \\ M_h &= \left\{q_h \in M \cap C^0(\Omega);\ q_h|_K \in P_1(K) \quad \forall K \in \Im_h\right\}, \end{aligned} \tag{2.11}$$

where $P_K = P_1(K)^2 \oplus \text{span}\{\lambda_{K1}\lambda_{K2}\lambda_{K3}\}^2$.

Example 2.3. The second-order finite element space $X_h \times M_h$ can be taken as

$$\begin{aligned} X_h &= \left\{\boldsymbol{v}_h \in X \cap C^0(\Omega)^2;\ \boldsymbol{v}_h|_K \in P_K \quad \forall K \in \Im_h\right\}, \\ M_h &= \left\{q_h \in M \cap C^0(\Omega);\ q_h|_K \in P_1(K) \quad \forall K \in \Im_h\right\}, \end{aligned} \tag{2.12}$$

where $P_K = P_2(K)^2 \oplus \text{span}\{\lambda_{K1}\lambda_{K2}\lambda_{K3}\}^2$.

Example 2.4. The third-order finite element space $X_h \times M_h$ can be taken as

$$\begin{aligned} X_h &= \left\{\boldsymbol{v}_h \in X \cap C^0(\Omega)^2;\ \boldsymbol{v}_h|_K \in P_K \quad \forall K \in \Im_h\right\}, \\ M_h &= \left\{q_h \in M \cap C^0(\Omega);\ q_h|_K \in P_2(K) \quad \forall K \in \Im_h\right\}, \end{aligned} \tag{2.13}$$

where $P_K = P_3(K)^2 \oplus \text{span}\{\lambda_{K1}\lambda_{K2}\lambda_{K3}\lambda_{Ki},\ i = 1,2,3\}^2$.

It has been proved (see [33]) that, for the finite element space $X_h \times M_h$ in Examples 2.1–2.4, there exists a restriction operator r_h: $X \to X_h$ such that, for any $\boldsymbol{v} \in X$,

$$
\begin{aligned}
&b(q_h, \boldsymbol{v} - r_h \boldsymbol{v}) = 0 \quad \forall q_h \in M_h, \ \|\nabla r_h \boldsymbol{v}\|_0 \le C \|\nabla \boldsymbol{v}\|_0, \\
&\|\nabla(\boldsymbol{v} - r_h \boldsymbol{v})\|_0 \le C h^k |\boldsymbol{v}|_{k+1} \ \text{ if } \boldsymbol{v} \in H^{k+1}(\Omega)^2, \quad k = 1, 2, 3.
\end{aligned} \tag{2.14}
$$

The spaces $X_h \times M_h$ used throughout the next part in this paper mean those in Examples 2.1–2.4, which satisfy the discrete LBB condition (2.9) (see [33] for a more detailed proof).

In order to find a numerical solution for Problem (II), it is necessary to discretize Problem (II). We introduce a MFE approximation for the spatial variable and FDS (finite difference scheme) for the time derivative. Let L be the positive integer, denote the time step increment by $k = T/L$ (T being the total time), $t^{(n)} = nk$, $0 \le n \le L$; $(\boldsymbol{u}_h^n, p_h^n) \in X_h \times M_h$ the MFE approximation corresponding to $(u(t^{(n)}), p(t^{(n)})) \equiv (\boldsymbol{u}^n, p^n)$. Then, applying a semi-implicit Euler scheme for the time integration, the fully discrete MFE solution for Problem (I) may be written as:

Problem (III) Find $(\boldsymbol{u}_h^n, p_h^n) \in X_h \times M_h$ such that

$$
\begin{cases}
(\boldsymbol{u}_h^n, \boldsymbol{v}_h) + ka(\boldsymbol{u}_h^n, \boldsymbol{v}_h) + ka_1\left(\boldsymbol{u}_h^{n-1}, \boldsymbol{u}_h^n, \boldsymbol{v}_h\right) - kb(p_h^n, \boldsymbol{v}_h) \\
\quad = k(f^n, \boldsymbol{v}_h) + \left(\boldsymbol{u}_h^{n-1}, \boldsymbol{v}_h\right) \quad \forall \boldsymbol{v}_h \in X_h, \\
b(q_h, \boldsymbol{u}_h^n) = 0 \qquad \forall q_h \in M_h, \\
\boldsymbol{u}_h^0 = \boldsymbol{0} \ \text{ in } \Omega,
\end{cases} \tag{2.15}
$$

where $1 \le n \le L$.

Put $A(\boldsymbol{u}_h^n, \boldsymbol{v}_h) = (\boldsymbol{u}_h^n, \boldsymbol{v}_h) + ka(\boldsymbol{u}_h^n, \boldsymbol{v}_h) + ka_1(\boldsymbol{u}_h^{n-1}, \boldsymbol{u}_h^n, \boldsymbol{v}_h)$. Since $A(\boldsymbol{u}_h^n, \boldsymbol{u}_h^n) = (\boldsymbol{u}_h^n, \boldsymbol{u}_h^n) + ka(\boldsymbol{u}_h^n, \boldsymbol{u}_h^n) + ka_1(\boldsymbol{u}_h^{n-1}, \boldsymbol{u}_h^n, \boldsymbol{u}_h^n) = \|\boldsymbol{u}_h^n\|_0 + k\nu \|\nabla \boldsymbol{u}_h^n\|_0$, $A(\cdot,\cdot)$ is coercive in $X_h \times X_h$. And $kb(\cdot,\cdot)$ also satisfies the discrete LBB condition in $X_h \times M_h$; therefore, by MFE theory (see [1], [32], or [33]), we obtain the following result.

THEOREM 2.2. *Under the assumptions* (2.8), (2.9), *if* $\boldsymbol{f} \in H^{-1}(\Omega)^2$ *satisfies* $N \sum_{i=1}^n \|\boldsymbol{f}^i\|_{-1} < \nu^2$, *then Problem* (III) *has a unique solution* $(\boldsymbol{u}_h^n, p_h^n) \in X_h \times M_h$ *and satisfies*

$$
\|\boldsymbol{u}_h^n\|_0^2 + k\nu \sum_{i=1}^n \|\nabla \boldsymbol{u}_h^i\|_0^2 \le k\nu^{-1} \sum_{i=1}^n \|\boldsymbol{f}^i\|_{-1}^2, \tag{2.16}
$$

if $k = O(h^2)$,

$$
\|\boldsymbol{u}^n - \boldsymbol{u}_h^n\|_0 + k^{1/2} \sum_{i=1}^n \|\nabla(\boldsymbol{u}^i - \boldsymbol{u}_h^i)\|_0 + k^{1/2} \sum_{i=1}^n \|p^i - p_h^i\|_0 \le C(h^m + k), \tag{2.17}
$$

where $(\boldsymbol{u}, p) \in [H_0^1(\Omega) \cap H^{m+1}(\Omega)]^2 \times [H^m(\Omega) \cap M]$ *is the exact solution for the problem* (I), *C is a constant dependent on* $|\boldsymbol{u}^n|_{m+1}$ *and* $|p^n|_m$, *and* $1 \le n \le L$.

If Reynolds number $Re = \nu^{-1}$, triangulation parameter h, finite element space $X_h \times M_h$, the time step increment k, and $\boldsymbol{f}$ are given, by solving Problem (III), we can obtain a solution ensemble $\{u_{1h}^n,\ u_{2h}^n,\ p_h^n\}_{n=1}^L$ for Problem (III). Then we choose ℓ (for example, $\ell = 20$, or 30, in general, $\ell \ll L$) instantaneous solutions $\boldsymbol{U}_i(x, y) = (u_{1h}^{n_i}, u_{2h}^{n_i}, p_h^{n_i})^T$ ($1 \le n_1 < n_2 < \cdots < n_\ell \le L$) (which are useful and of interest for us) from the L group of solutions $(u_{1h}^n,\ u_{2h}^n,\ p_h^n)^T$ ($1 \le n \le L$) for Problem (III), which are referred to as snapshots.

3. A reduced MFE formulation based POD technique for the nonstationary Navier–Stokes equations. In this section, we use the POD technique to deal with the snapshots in section 2 and produce an optimal representation in an average sense.

Recall $\hat{X}_h = X_h \times M_h$. For $\boldsymbol{U}_i(x, y) = (u_{1h}^{n_i}, u_{2h}^{n_i}, p_h^{n_i})^T$ $(i = 1, 2, \ldots, \ell)$ in section 2, we set

$$\mathcal{V} = \text{span}\{\boldsymbol{U}_1, \boldsymbol{U}_2, \ldots, \boldsymbol{U}_\ell\}, \tag{3.1}$$

and refer to $\mathcal{V}$ as the ensemble consisting of the snapshots $\{\boldsymbol{U}_i\}_{i=1}^{\ell}$, at least one of which is assumed to be nonzero. Let $\{\boldsymbol{\psi}_j\}_{j=1}^{l}$ denote an orthonormal basis of $\mathcal{V}$ with $l = \dim \mathcal{V}$. Then each member of the ensemble can expressed as

$$\boldsymbol{U}_i = \sum_{j=1}^{l} (\boldsymbol{U}_i, \boldsymbol{\psi}_j)_{\hat{X}} \boldsymbol{\psi}_j \quad \text{for} \quad i = 1, 2, \ldots, \ell, \tag{3.2}$$

where $(\boldsymbol{U}_i, \boldsymbol{\psi}_j)_{\hat{X}} \boldsymbol{\psi}_j = ((\nabla \boldsymbol{u}_h^{n_i}, \nabla \boldsymbol{\psi}_{uj})_0 \boldsymbol{\psi}_{uj}, (p_h^{n_i}, \psi_{pj})_0 \psi_{pj})$, $(\cdot, \cdot)_0$ is L^2-inner product, and $\boldsymbol{\psi}_{uj}$ and ψ_{pj} are orthonormal bases corresponding to $\boldsymbol{u}$ and p, respectively.

Since $\mathcal{V} = \text{span}\{\boldsymbol{U}_1, \boldsymbol{U}_2, \ldots, \boldsymbol{U}_\ell\} = \text{span}\{\boldsymbol{\psi}_1, \boldsymbol{\psi}_2, \ldots, \boldsymbol{\psi}_l\}$, $b(p_h^{n_i}, \boldsymbol{u}_h^{n_j}) = 0$ $(1 \le i, j \le \ell)$ implies $b(\psi_{pi}, \boldsymbol{\psi}_{uj}) = 0$ $(1 \le i, j \le l)$.

Definition 3.1. *The method of POD consists in finding the orthonormal basis such that for every d $(1 \le d \le l)$ the mean square error between the elements $\boldsymbol{U}_i$ $(1 \le i \le \ell)$ and corresponding dth partial sum of* (3.2) *is minimized on average:*

$$\min_{\{\boldsymbol{\psi}_j\}_{j=1}^{d}} \frac{1}{\ell} \sum_{i=1}^{\ell} \|\boldsymbol{U}_i - \sum_{j=1}^{d} (\boldsymbol{U}_i, \boldsymbol{\psi}_j)_{\hat{X}} \boldsymbol{\psi}_j\|_{\hat{X}}^2 \tag{3.3}$$

such that

$$(\boldsymbol{\psi}_i, \boldsymbol{\psi}_j)_{\hat{X}} = \delta_{ij} \quad \text{for } 1 \le i \le d, 1 \le j \le i, \tag{3.4}$$

where $\|\boldsymbol{U}_i\|_{\hat{X}} = [\|\nabla u_{1h}^{n_i}\|_0^2 + \|\nabla u_{2h}^{n_i}\|_0^2 + \|p_h^{n_i}\|_0^2]^{\frac{1}{2}}$. *A solution* $\{\boldsymbol{\psi}_j\}_{j=1}^{d}$ *of* (3.3) *and* (3.4) *is known as a POD basis of rank d.*

We introduce the correlation matrix $\boldsymbol{K} = (K_{ij})_{\ell \times \ell} \in R^{\ell \times \ell}$ corresponding to the snapshots $\{\boldsymbol{U}_i\}_{i=1}^{\ell}$ by

$$K_{ij} = \frac{1}{\ell} (\boldsymbol{U}_i, \boldsymbol{U}_j)_{\hat{X}}. \tag{3.5}$$

The matrix $\boldsymbol{K}$ is positive semidefinite and has rank l. The solutions of (3.3) and (3.4) can be found in [10], [15], or [28], for example.

Proposition 3.2. *Let $\lambda_1 \ge \lambda_2 \ge \cdots \ge \lambda_l > 0$ denote the positive eigenvalues of $\boldsymbol{K}$ and $\boldsymbol{v}_1, \boldsymbol{v}_2, \ldots, \boldsymbol{v}_l$ the associated orthonormal eigenvectors. Then a POD basis of rank $d \le l$ is given by*

$$\boldsymbol{\psi}_i = \frac{1}{\sqrt{\lambda_i}} \sum_{j=1}^{\ell} (\boldsymbol{v}_i)_j \boldsymbol{U}_j, \tag{3.6}$$

where $(\boldsymbol{v}_i)_j$ denotes the jth component of the eigenvector $\boldsymbol{v}_i$. Furthermore, the following error formula holds:

$$\frac{1}{\ell} \sum_{i=1}^{\ell} \left\| \boldsymbol{U}_i - \sum_{j=1}^{d} (\boldsymbol{U}_i, \boldsymbol{\psi}_j)_{\hat{X}} \boldsymbol{\psi}_j \right\|_{\hat{X}}^2 = \sum_{j=d+1}^{l} \lambda_j. \tag{3.7}$$

Let $\mathcal{V}^d = \text{span}\{\boldsymbol{\psi}_1, \boldsymbol{\psi}_2, \ldots, \boldsymbol{\psi}_d\}$ and $X^d \times M^d = \mathcal{V}^d$ with $X^d \subset X_h \subset X$ and $M^d \subset M_h \subset M$. Set the Ritz-projection P^h: $X \to X_h$ (if P^h is restricted to Ritz-projection from X_h to X^d, it is written as P^d) such that $P^h|_{X_h} = P^d : X_h \to X^d$ and $P^h : X\backslash X_h \to X_h\backslash X^d$ and L^2-projection ρ^d: $M \to M^d$ denoted by, respectively,

$$a(P^h\boldsymbol{u}, \boldsymbol{v}_h) = a(\boldsymbol{u}, \boldsymbol{v}_h) \quad \forall \boldsymbol{v}_h \in X_h \tag{3.8}$$

and

$$(\rho^d p, q_d)_0 = (p, q_d)_0 \quad \forall q_d \in M^d, \tag{3.9}$$

where $\boldsymbol{u} \in X$ and $p \in M$. Due to (3.8) and (3.9) the linear operators P^h and ρ^d are well-defined and bounded:

$$\|\nabla(P^d\boldsymbol{u})\|_0 \le \|\nabla\boldsymbol{u}\|_0, \quad \|\rho^d p\|_0 \le \|p\|_0 \quad \forall \boldsymbol{u} \in X \text{ and } p \in M. \tag{3.10}$$

LEMMA 3.3. *For every d $(1 \le d \le l)$ the projection operators P^d and ρ^d satisfy, respectively,*

$$\frac{1}{\ell}\sum_{i=1}^{\ell} \|\nabla(\boldsymbol{u}_h^{n_i} - P^d\boldsymbol{u}_h^{n_i})\|_0^2 \le \sum_{j=d+1}^{l} \lambda_j, \tag{3.11}$$

$$\frac{1}{\ell}\sum_{i=1}^{\ell} \|\boldsymbol{u}_h^{n_i} - P^d\boldsymbol{u}_h^{n_i}\|_0^2 \le Ch^2 \sum_{j=d+1}^{l} \lambda_j, \tag{3.12}$$

and

$$\frac{1}{\ell}\sum_{i=1}^{\ell} \|p_h^{n_i} - \rho^d p_h^{n_i}\|_0^2 \le \sum_{j=d+1}^{l} \lambda_j, \tag{3.13}$$

where $\boldsymbol{u}_h^{n_i} = (u_{1h}^{n_i}, u_{2h}^{n_i})$ and $(u_{1h}^{n_i}, u_{2h}^{n_i}, p_h^{n_i})^T \in \mathcal{V}$.

Proof. For any $\boldsymbol{u} \in X$ we deduce from (3.8) that

$$\begin{aligned}\nu\|\nabla(\boldsymbol{u} - P^h\boldsymbol{u})\|_0^2 &= a(\boldsymbol{u} - P^h\boldsymbol{u}, \boldsymbol{u} - P^h\boldsymbol{u}) \\ &= a(\boldsymbol{u} - P^h\boldsymbol{u}, \boldsymbol{u} - \boldsymbol{v}_h) \\ &\le \nu\|\nabla(\boldsymbol{u} - P^h\boldsymbol{u})\|_0 \|\nabla(\boldsymbol{u} - \boldsymbol{v}_h)\|_0 \quad \forall \boldsymbol{v}_h \in X_h.\end{aligned}$$

Therefore, we obtain that

$$\|\nabla(\boldsymbol{u} - P^h\boldsymbol{u})\|_0 \le \|\nabla(\boldsymbol{u} - \boldsymbol{v}_h)\|_0 \quad \forall \boldsymbol{v}_h \in X_h. \tag{3.14}$$

If $\boldsymbol{u} = \boldsymbol{u}_h^{n_i}$, and P^h is restricted to Ritz-projection from X_h to X^d, i.e., $P^h\boldsymbol{u}_h^{n_i} = P^d\boldsymbol{u}_h^{n_i} \in X^d$, taking $\boldsymbol{v}_h = \sum_{j=1}^{d}(\boldsymbol{u}_h^{n_i}, \boldsymbol{\psi}_{uj})_X \boldsymbol{\psi}_{uj} \in X^d \subset X_h$ (where $\boldsymbol{\psi}_{uj}$ is the component of $\boldsymbol{\psi}_j$ corresponding to $\boldsymbol{u}$) in (3.14), we can obtain (3.11) from (3.7).

In order to prove (3.12), we consider the following variational problem:

$$(\nabla\boldsymbol{w}, \nabla\boldsymbol{v}) = (\boldsymbol{u} - P^h\boldsymbol{u}, \boldsymbol{v}) \quad \forall \boldsymbol{v} \in X. \tag{3.15}$$

Thus, $\boldsymbol{w} \in [H_0^1(\Omega) \cap H^2(\Omega)]^2$ and satisfies $\|\boldsymbol{w}\|_2 \le C\|\boldsymbol{u} - P^h\boldsymbol{u}\|_0$. Taking $\boldsymbol{v} = \boldsymbol{u} - P^h\boldsymbol{u}$ in (3.15), from (3.14) we obtain that

$$\begin{aligned}\|\boldsymbol{u} - P^h\boldsymbol{u}\|_0^2 &= (\nabla\boldsymbol{w}, \nabla(\boldsymbol{u} - P^h\boldsymbol{u})) \\ &= (\nabla(\boldsymbol{w} - \boldsymbol{w}_h), \nabla(\boldsymbol{u} - P^h\boldsymbol{u})) \\ &\le \|\nabla(\boldsymbol{w} - \boldsymbol{w}_h)\|_0 \|\nabla(\boldsymbol{u} - P^d\boldsymbol{u})\|_0 \quad \forall \boldsymbol{w}_h \in X_h.\end{aligned} \tag{3.16}$$

Taking $\boldsymbol{w}_h = r_h\boldsymbol{w}$, from (2.14) and (3.16) we have

$$\begin{aligned}\|\boldsymbol{u} - P^h\boldsymbol{u}\|_0^2 &\le Ch\|\boldsymbol{w}\|_2\|\nabla(\boldsymbol{u} - P^h\boldsymbol{u})\|_0\\ &\le Ch\|\boldsymbol{u} - P^h\boldsymbol{u}\|_0\|\nabla(\boldsymbol{u} - P^h\boldsymbol{u})\|_0.\end{aligned}$$

Thus, we obtain that

$$\|\boldsymbol{u} - P^h\boldsymbol{u}\|_0 \le Ch\|\nabla(\boldsymbol{u} - P^h\boldsymbol{u})\|_0. \tag{3.17}$$

Therefore, if $\boldsymbol{u} = \boldsymbol{u}_h^{n_i}$ and P^h is restricted to Ritz-projection from X_h to X^d, i.e., $P^h\boldsymbol{u}_h^{n_i} = P^d\boldsymbol{u}_h^{n_i} \in X^d$, by (3.17) and (3.11) we obtain (3.12).

Using Hölder inequality and (3.9) can yield

$$\begin{aligned}\|p_h^{n_i} - \rho^d p_h^{n_i}\|_0^2 &= (p_h^{n_i} - \rho^d p_h^{n_i}, p_h^{n_i} - \rho^d p_h^{n_i})\\ &= (p_h^{n_i} - \rho^d p_h^{n_i}, p_h^{n_i} - q_d)\\ &\le \|p_h^{n_i} - \rho^d p_h^{n_i}\|_0\|p_h^{n_i} - q_d\|_0 \quad \forall q_d \in M^d,\end{aligned}$$

and consequently,

$$\|p_h^{n_i} - \rho^d p_h^{n_i}\|_0 \le \|p_h^{n_i} - q_d\|_0 \quad \forall q_d \in M^d. \tag{3.18}$$

Taking $q_d = \sum_{j=1}^d (p_h^{n_i}, \psi_{pj})_0\psi_{pj}$ (where ψ_{pj} is the component of $\boldsymbol{\psi}_j$ corresponding to p) in (3.18), from (3.7) we can obtain (3.13), which completes the proof of Lemma 3.3. ◻

Thus, using $\mathcal{V}^d = X^d \times M^d$, we can obtain the reduced formulation for Problem (III) as follows.

Problem (IV) Find $(\boldsymbol{u}_d^n, p_d^n) \in \mathcal{V}^d$ such that

$$\begin{cases} (\boldsymbol{u}_d^n, \boldsymbol{v}_d) + ka(\boldsymbol{u}_d^n, \boldsymbol{v}_d) + ka_1\left(\boldsymbol{u}_d^{n-1}, \boldsymbol{u}_d^n, \boldsymbol{v}_d\right) - kb(p_d^n, \boldsymbol{v}_d)\\ \quad = k(f^n, \boldsymbol{v}_d) + \left(\boldsymbol{u}_d^{n-1}, \boldsymbol{v}_d\right) \quad \forall \boldsymbol{v}_d \in X^d,\\ b(q_d, \boldsymbol{u}_d^n) = 0 \quad \forall q_d \in M^d,\\ \boldsymbol{u}_d^0 = \boldsymbol{0}, \end{cases} \tag{3.19}$$

where $1 \le n \le L$.

Remark 3.4. Problem (IV) is a reduced MFE formulation based on the POD technique for Problem (III), since it includes only $3d$ ($d \ll l \le \ell \ll L$) degrees of freedom and is independent of the spatial grid scale h, while Problem (III) includes $3N_p+N_K \approx 5N_p$ for Mini's element of Example 2.2 (where N_p is the number of vertices in $\Im_h$ and N_K the number of elements in $\Im_h$) and $3d \ll 5N_p$ (for example, in section 5, $d \le 7$, while $N_p = 32\times 32 = 1024$). The number of degrees of freedom of Example 2.1 is also approximately $5N_p$, but Example 2.3 and Example 2.4 are more. When one computes actual problems, one may obtain the ensemble of snapshots from physical system trajectories by drawing samples from experiments and interpolation (or data assimilation). For example, for weather forecast, one can use the previous weather prediction results to construct the ensemble of snapshots, and then restructure the POD basis for the ensemble of snapshots by above (3.3)–(3.6), and finally combine it with a Galerkin projection to derive a reduced order dynamical system; i.e., one needs only to solve the above Problem (IV), which has only $3d$ degrees of freedom, but it is unnecessary to solve Problem (III). Thus, the forecast of future weather change can be quickly simulated, which is a result of major importance for real-life applications. Since the development and change of a large number of future nature phenomena are closely related to previous results (for example, weather change, biology anagenesis, and so on), using existing results as snapshots in order to structure POD basis, by solving corresponding PDEs, one may truly capture the laws of change of natural phenomena. Therefore, these POD methods provide useful and important applications.

4. Existence and error analysis of the solution of the reduced MFE formulation based on POD technique for the nonstationary Navier–Stokes equations. This section is devoted to discussing the existence and error estimates for Problem (IV).

We see from (3.6) that $\mathcal{V}^d = X^d \times M^d \subset \mathcal{V} \subset X_h \times M_h \subset X \times M$, where $X_h \times M_h$ is one of those spaces in Examples 2.1–2.4. Therefore, we have in the following result.

LEMMA 4.1. *There exists also an operator r_d: $X_h \rightarrow X^d$ such that, for all $\boldsymbol{u}_h \in X_h$,*

$$b(q_d, \boldsymbol{u}_h - r_d\boldsymbol{u}_h) = 0 \quad \forall q_d \in M^d, \ \|\nabla r_d\boldsymbol{u}_h\|_0 \le c\|\nabla \boldsymbol{u}_h\|_0, \tag{4.1}$$

and, for every d $(1 \le d \le l)$,

$$\frac{1}{\ell}\sum_{i=1}^{\ell} \|\nabla(\boldsymbol{u}_h^{n_i} - r_d\boldsymbol{u}_h^{n_i})\|_0^2 \le C \sum_{j=d+1}^{l} \lambda_j. \tag{4.2}$$

Proof. We use the Mini's and the second finite element as examples. Noting that for any $q_d \in M^d$ and $K \in \Im_h$, $\nabla q_d|_K \in P_0(K)$, using Green formula, we have

$$\begin{aligned} b(q_d, \boldsymbol{u}_h - r_d\boldsymbol{u}_h) &= -\int_\Omega \nabla q_d(\boldsymbol{u}_h - r_d\boldsymbol{u}_h)\mathrm{d}x\mathrm{d}y \\ &= -\sum_{K\in\Im_h} \nabla q_d|_K \int_K (\boldsymbol{u}_h - r_d\boldsymbol{u}_h)\mathrm{d}x\mathrm{d}y. \end{aligned}$$

Define r_d as follows:

$$r_d\boldsymbol{u}_h|_K = P^d\boldsymbol{u}_h|_K + \gamma_K\lambda_{K1}\lambda_{K2}\lambda_{K3} \quad \forall \boldsymbol{v}_h \in X_h \text{ and } K \in \Im_h, \tag{4.3}$$

where $\gamma_K = \int_K(\boldsymbol{u}_h - P^d\boldsymbol{u}_h)\mathrm{d}x / \int_K \lambda_{K1}\lambda_{K2}\lambda_{K3}\mathrm{d}x$. Thus, the first equality of (4.1) holds. Using (3.10)–(3.12) yields the inequality of (4.1). Then, if $\boldsymbol{u}_h = \boldsymbol{u}_h^{n_i}$, using (3.11)–(3.12), by simply computing we deduce (4.2). ∎

Set

$$\begin{aligned} V &= \{\boldsymbol{v} \in X;\ b(q, \boldsymbol{v}) = 0 \ \ \forall q \in M\}, \\ V_h &= \{\boldsymbol{v}_h \in X_h;\ b(q_h, \boldsymbol{v}_h) = 0 \ \ \forall q_h \in M_h\}, \\ V^d &= \{\boldsymbol{v}_d \in X^d;\ b(q_d, \boldsymbol{v}_d) = 0 \ \ \forall q_d \in M^d\}. \end{aligned}$$

Using dual principle and inequalities (3.11) and (3.12), we deduce the following result (see [1], [31]–[33]).

LEMMA 4.2. *There exists an operator R_d: $V \cup V_h \rightarrow V^d$ such that, for all $\boldsymbol{v} \in V \cup V_h$,*

$$(\boldsymbol{v} - R_d\boldsymbol{v}, \boldsymbol{v}_d) = 0 \quad \forall \boldsymbol{v}_d \in V^d, \ \|\nabla R_d\boldsymbol{v}\|_0 \le C\|\nabla \boldsymbol{v}\|_0,$$

and, for every d $(1 \le d \le l)$,

$$\frac{1}{\ell}\sum_{i=1}^{\ell}\|\boldsymbol{u}_h^{n_i}-R_d\boldsymbol{u}_h^{n_i}\|_{-1}^2 \le \frac{Ch^2}{\ell}\sum_{i=1}^{\ell}\|\nabla(\boldsymbol{u}_h^{n_i}-R_d\boldsymbol{u}_h^{n_i})\|_0^2 \le Ch^2\sum_{j=d+1}^{l}\lambda_j, \tag{4.4}$$

where $\|\cdot\|_{-1}$ denotes the normal of space $H^{-1}(\Omega)^2$ (see (2.7)).

We have the following result for the solution of Problem (IV).

THEOREM 4.3. *Under the hypotheses of Theorem 2.2, Problem (IV) has a unique solution $(\boldsymbol{u}_d^n, p_d^n) \in X^d \times M^d$ and satisfies*

$$\|\boldsymbol{u}_d^n\|_0^2 + k\nu\sum_{i=1}^{n}\|\nabla\boldsymbol{u}_d^i\|_0^2 \le k\nu^{-1}\sum_{i=1}^{n}\|f^i\|_{-1}^2. \tag{4.5}$$

Proof. Using the same technique as the proof of Theorem 2.2, we could prove that Problem (IV) has a unique solution $(\boldsymbol{u}_d^n, p_d^n) \in X^d \times M^d$ and satisfies (4.5). ∎

In the following theorem, error estimates of the solution for Problem (IV) are derived.

THEOREM 4.4. *Under the hypotheses of Theorem 2.2, if $h^2 = O(k)$, $k = O(\ell^{-2})$, snapshots are equably taken, and $\boldsymbol{f} \in H^{-1}(\Omega)^2$ satisfies $2\nu^{-2}N\sum_{i=1}^{n}\|\boldsymbol{f}^i\|_{-1} < 1$, then the error between the solution $(\boldsymbol{u}_d^n, p_d^n)$ for Problem (IV) and the solution $(\boldsymbol{u}_h^n, p_h^n)$ for Problem (III) has the following error estimates, for $n = 1, 2, \ldots, L$,*

$$\begin{aligned}
&\|\boldsymbol{u}_h^{n_i}-\boldsymbol{u}_d^{n_i}\|_0 + k^{1/2}\|p_h^{n_i}-p_d^{n_i}\|_0 + k^{1/2}\|\nabla(\boldsymbol{u}_h^{n_i}-\boldsymbol{u}_d^{n_i})\|_0\\
&\le C\left(k^{1/2}\sum_{j=d+1}^{l}\lambda_j\right)^{1/2}, \quad i = 1, 2, \ldots, \ell;\\
&\|\boldsymbol{u}_h^{n}-\boldsymbol{u}_d^{n}\|_0 + k^{1/2}\|p_h^{n}-p_d^{n}\|_0 + k^{1/2}\|\nabla(\boldsymbol{u}_h^{n}-\boldsymbol{u}_d^{n})\|_0\\
&\le Ck + C\left(k^{1/2}\sum_{j=d+1}^{l}\lambda_j\right)^{1/2}, \quad n \notin \{n_1, n_2, \ldots, n_\ell\}.
\end{aligned} \tag{4.6}$$

Proof. Subtracting Problem (IV) from Problem (III), taking $\boldsymbol{v}_h = \boldsymbol{v}_d \in X^d$ and $q_h = q_d \in M^d$, can yield

$$\begin{aligned}
&(\boldsymbol{u}_h^n-\boldsymbol{u}_d^n, \boldsymbol{v}_d) + ka(\boldsymbol{u}_h^n-\boldsymbol{u}_d^n, \boldsymbol{v}_d) - kb(p_h^n-p_d^n, \boldsymbol{v}_d) + ka_1\left(\boldsymbol{u}_h^{n-1}, \boldsymbol{u}_h^n, \boldsymbol{v}_d\right)\\
&-ka_1\left(\boldsymbol{u}_d^{n-1}, \boldsymbol{u}_d^n, \boldsymbol{v}_d\right) = \left(\boldsymbol{u}_h^{n-1}-\boldsymbol{u}_d^{n-1}, \boldsymbol{v}_d\right) \quad \forall \boldsymbol{v}_d \in X^d,
\end{aligned} \tag{4.7}$$

$$b(q_d, \boldsymbol{u}_h^n-\boldsymbol{u}_d^n) = 0 \quad \forall q_d \in M^d, \tag{4.8}$$

$$\boldsymbol{u}_h^0-\boldsymbol{u}_d^0 = \boldsymbol{0}. \tag{4.9}$$

We obtain, from (2.3), (2.7), Theorem 2.2, and Theorem 4.3, by Hölder inequality, that

$$\begin{aligned}
&|a_1\left(\boldsymbol{u}_h^{n-1}, \boldsymbol{u}_h^n, \boldsymbol{v}_d\right) - a_1\left(\boldsymbol{u}_d^{n-1}, \boldsymbol{u}_d^n, \boldsymbol{v}_d\right)|\\
&= |a_1\left(\boldsymbol{u}_h^{n-1}-\boldsymbol{u}_d^{n-1}, \boldsymbol{u}_h^n, \boldsymbol{v}_d\right) + a_1\left(\boldsymbol{u}_d^{n-1}, \boldsymbol{u}_h^n-\boldsymbol{u}_d^n, \boldsymbol{v}_d\right)|\\
&\le C[\|\nabla\left(\boldsymbol{u}_h^{n-1}-\boldsymbol{u}_d^{n-1}\right)\|_0 + \|\nabla(\boldsymbol{u}_h^n-\boldsymbol{u}_d^n)\|_0]\|\nabla\boldsymbol{v}_d\|_0,
\end{aligned} \tag{4.10}$$

especially, if $\boldsymbol{v}_d = P^d\boldsymbol{u}_h^n - \boldsymbol{u}_d^n$, then

$$
\begin{aligned}
&|a_1\left(\boldsymbol{u}_h^{n-1}, \boldsymbol{u}_h^n, P^d\boldsymbol{u}_h^n - \boldsymbol{u}_d^n\right) - a_1\left(\boldsymbol{u}_d^{n-1}, \boldsymbol{u}_d^n, P^d\boldsymbol{u}_h^n - \boldsymbol{u}_d^n\right)| \\
&= |a_1\left(\boldsymbol{u}_h^{n-1} - \boldsymbol{u}_d^{n-1}, \boldsymbol{u}_h^n, P^d\boldsymbol{u}_h^n - \boldsymbol{u}_d^n\right) + a_1\left(\boldsymbol{u}_d^{n-1}, \boldsymbol{u}_h^n - \boldsymbol{u}_d^n, P^d\boldsymbol{u}_h^n - \boldsymbol{u}_d^n\right)| \\
&= |a_1\left(\boldsymbol{u}_h^{n-1} - \boldsymbol{u}_d^{n-1}, \boldsymbol{u}_h^n, P^d\boldsymbol{u}_h^n - \boldsymbol{u}_h^n\right) + a_1\left(\boldsymbol{u}_h^{n-1} - \boldsymbol{u}_d^{n-1}, \boldsymbol{u}_h^n, \boldsymbol{u}_h^n - \boldsymbol{u}_d^n\right) \\
&\quad + a_1\left(\boldsymbol{u}_d^{n-1}, \boldsymbol{u}_h^n - \boldsymbol{u}_d^n, P^d\boldsymbol{u}_h^n - \boldsymbol{u}_h^n\right)| \\
&\le C\|\nabla(\boldsymbol{u}_h^n - P^d\boldsymbol{u}_h^n)\|_0^2 + \varepsilon[\|\nabla\left(\boldsymbol{u}_h^{n-1} - \boldsymbol{u}_d^{n-1}\right)\|_0^2 + \|\nabla(\boldsymbol{u}_h^n - \boldsymbol{u}_d^n)\|_0^2] \\
&\quad + N\|\nabla\boldsymbol{u}_h^n\|_0\|\nabla\left(\boldsymbol{u}_h^{n-1} - \boldsymbol{u}_d^{n-1}\right)\|_0\|\nabla(\boldsymbol{u}_h^n - \boldsymbol{u}_d^n)\|_0,
\end{aligned} \tag{4.11}
$$

where ε is a small positive constant which can be chosen arbitrarily.

Write $\bar{\partial}_t\boldsymbol{u}_h^n = [\boldsymbol{u}_h^n - \boldsymbol{u}_h^{n-1}]/k$ and note that $\bar{\partial}_t\boldsymbol{u}_d^n \in V^d$ and $\bar{\partial}_t R_d\boldsymbol{u}_n^n \in V^d$. From Lemma 4.2, (4.7), and (4.10), we have that

$$
\begin{aligned}
&\|\bar{\partial}_t\boldsymbol{u}_h^n - \bar{\partial}_t\boldsymbol{u}_d^n\|_{-1} \le \|\bar{\partial}_t\boldsymbol{u}_h^n - \bar{\partial}_t R_d\boldsymbol{u}_h^n\|_{-1} + \|\bar{\partial}_t R_h\boldsymbol{u}_h^n - \bar{\partial}_t\boldsymbol{u}_d^n\|_{-1} \\
&\le \|\bar{\partial}_t\boldsymbol{u}_h^n - \bar{\partial}_t R_d\boldsymbol{u}_h^n\|_{-1} + \sup_{\boldsymbol{v}\in V}\frac{\left(\bar{\partial}_t R_d\boldsymbol{u}_h^n - \bar{\partial}_t\boldsymbol{u}_d^n, \boldsymbol{v}\right)}{\|\nabla\boldsymbol{v}\|_0} \\
&= \|\bar{\partial}_t\boldsymbol{u}_h^n - \bar{\partial}_t R_d\boldsymbol{u}_h^n\|_{-1} + \sup_{\boldsymbol{v}\in V}\frac{\left(\bar{\partial}_t\boldsymbol{u}_h^n - \bar{\partial}_t\boldsymbol{u}_d^n, R_d\boldsymbol{v}\right)}{\|\nabla\boldsymbol{v}\|_0} \\
&= \|\bar{\partial}_t\boldsymbol{u}_h^n - \bar{\partial}_t R_d\boldsymbol{u}_h^n\|_{-1} + \sup_{\boldsymbol{v}\in V}\frac{1}{\|\nabla\boldsymbol{v}\|_0}\big[b\left(p_h^n - p_d^n, R_d\boldsymbol{v}\right) \\
&\quad -a(\boldsymbol{u}_h^n - \boldsymbol{u}_d^n, R_d\boldsymbol{v}) - a_1\left(\boldsymbol{u}_h^{n-1}, \boldsymbol{u}_h^n, R_d\boldsymbol{v}\right) + a_1\left(\boldsymbol{u}_d^{n-1}, \boldsymbol{u}_d^n, R_d\boldsymbol{v}\right)\big] \\
&= \|\bar{\partial}_t\boldsymbol{u}_h^n - \bar{\partial}_t R_d\boldsymbol{u}_h^n\|_{-1} + \sup_{\boldsymbol{v}\in V}\frac{1}{\|\nabla\boldsymbol{v}\|_0}\big[b\left(p_h^n - \rho^d p_h^n, R_d\boldsymbol{v}\right) \\
&\quad -a(\boldsymbol{u}_h^n - \boldsymbol{u}_d^n, R_d\boldsymbol{v}) - a_1\left(\boldsymbol{u}_h^{n-1}, \boldsymbol{u}_h^n, R_d\boldsymbol{v}\right) + a_1\left(\boldsymbol{u}_d^{n-1}, \boldsymbol{u}_d^n, R_d\boldsymbol{v}\right)\big] \\
&\le \|\bar{\partial}_t\boldsymbol{u}_h^n - \bar{\partial}_t R_d\boldsymbol{u}_h^n\|_{-1} + C\big[\|p_h^n - \rho^d p_h^n\|_0 \\
&\quad + \|\nabla\left(\boldsymbol{u}_h^{n-1} - \boldsymbol{u}_d^{n-1}\right)\|_0 + \|\nabla(\boldsymbol{u}_h^n - \boldsymbol{u}_d^n)\|_0\big].
\end{aligned} \tag{4.12}
$$

By using (2.9), (4.7), (4.10), (4.12), and Lemma 4.1, we have that

$$
\begin{aligned}
&\beta\|\rho^d p_h^n - p_d^n\|_0 \le \sup_{\boldsymbol{v}_h\in X_h}\frac{b(\rho^d p_h^n - p_d^n, \boldsymbol{v}_h)}{\|\nabla\boldsymbol{v}_h\|_0} = \sup_{\boldsymbol{v}_h\in X_h}\frac{b(p_h^n - p_d^n, r_d\boldsymbol{v}_h)}{\|\nabla\boldsymbol{v}_h\|_0} \\
&= \sup_{\boldsymbol{v}_h\in X_h}\frac{1}{\|\nabla\boldsymbol{v}_h\|_0}\big[\left(\bar{\partial}_t\boldsymbol{u}_h^n - \bar{\partial}_t\boldsymbol{u}_d^n, r_d\boldsymbol{v}_h\right) + a(\boldsymbol{u}_h^n - \boldsymbol{u}_d^n, r_d\boldsymbol{v}) \\
&\quad + a_1\left(\boldsymbol{u}_h^{n-1}, \boldsymbol{u}_h^n, r_d\boldsymbol{v}\right) - a_1\left(\boldsymbol{u}_d^{n-1}, \boldsymbol{u}_d^n, r_d\boldsymbol{v}\right)\big] \\
&\le C\left[\|\bar{\partial}_t\boldsymbol{u}_h^n - \bar{\partial}_t\boldsymbol{u}_d^n\|_{-1} + \|\nabla\left(\boldsymbol{u}_h^{n-1} - \boldsymbol{u}_d^{n-1}\right)\|_0 + \|\nabla(\boldsymbol{u}_h^n - \boldsymbol{u}_d^n)\|_0\right] \\
&\le C\big[\|\bar{\partial}_t\boldsymbol{u}_h^n - \bar{\partial}_t R_d\boldsymbol{u}_h^n\|_{-1} + \|p_h^n - \rho^d p_h^n\|_0 \\
&\quad + \|\nabla\left(\boldsymbol{u}_h^{n-1} - \boldsymbol{u}_d^{n-1}\right)\|_0 + \|\nabla(\boldsymbol{u}_h^n - \boldsymbol{u}_d^n)\|_0\big].
\end{aligned} \tag{4.13}
$$

Thus, we obtain that

$$
\begin{aligned}
&\|p_h^n - p_d^n\|_0 \le \|p_h^n - \rho^d p_h^n\|_0 + \|\rho^d p_h^n - p_d^n\|_0 \le C[\|\nabla\left(\boldsymbol{u}_h^{n-1} - \boldsymbol{u}_d^{n-1}\right)\|_0 \\
&\quad + \|\nabla(\boldsymbol{u}_h^n - \boldsymbol{u}_d^n)\|_0 + \|\bar{\partial}_t\boldsymbol{u}_h^n - \bar{\partial}_t R_d\boldsymbol{u}_h^n\|_{-1} + \|p_h^n - \rho^d p_h^n\|_0].
\end{aligned} \tag{4.14}
$$

Taking $\boldsymbol{v}_d = P^d \boldsymbol{u}_h^n - \boldsymbol{u}_d^n$ in (4.7), it follows from (4.8) that

(4.15)
$$\begin{aligned}
&(\boldsymbol{u}_h^n - \boldsymbol{u}_d^n, \boldsymbol{u}_h^n - \boldsymbol{u}_d^n) - \left(\boldsymbol{u}_h^{n-1} - \boldsymbol{u}_d^{n-1}, \boldsymbol{u}_h^n - \boldsymbol{u}_d^n\right) + ka(\boldsymbol{u}_h^n - \boldsymbol{u}_d^n, \boldsymbol{u}_h^n - \boldsymbol{u}_d^n) \\
&= \left(\boldsymbol{u}_h^n - \boldsymbol{u}_d^n - \left(\boldsymbol{u}_h^{n-1} - \boldsymbol{u}_d^{n-1}\right), \boldsymbol{u}_h^n - P^d \boldsymbol{u}_h^n\right) + ka\left(\boldsymbol{u}_h^n - P^d \boldsymbol{u}_h^n, \boldsymbol{u}_h^n - P^d \boldsymbol{u}_h^n\right) \\
&\quad + kb\left(p_h^n - \rho^d p_h^n, \boldsymbol{u}_h^n - \boldsymbol{u}_d^n\right) + kb\left(p_h^n - p_d^n, \boldsymbol{u}_h^n - P^d \boldsymbol{u}_h^n\right) \\
&\quad - ka_1\left(\boldsymbol{u}_h^{n-1}, \boldsymbol{u}_h^n, P^d \boldsymbol{u}_h^n - \boldsymbol{u}_d^n\right) + ka_1\left(\boldsymbol{u}_d^{n-1}, \boldsymbol{u}_d^n, P^d \boldsymbol{u}_h^n - \boldsymbol{u}_d^n\right).
\end{aligned}$$

Thus, noting that $a(a-b) = [a^2 - b^2 + (a-b)^2]/2$ (for $a \geq 0$ and $b \geq 0$), by (4.11), (4.14), Hölder inequality, Cauchy inequality, and Proposition 3.2, we obtain that

(4.16)
$$\begin{aligned}
&\frac{1}{2}\left[\|\boldsymbol{u}_h^n - \boldsymbol{u}_d^n\|_0^2 - \|\boldsymbol{u}_h^{n-1} - \boldsymbol{u}_d^{n-1}\|_0^2 + \|\boldsymbol{u}_h^n - \boldsymbol{u}_d^n - \left(\boldsymbol{u}_h^{n-1} - \boldsymbol{u}_d^{n-1}\right)\|_0^2\right] \\
&+ \nu k\|\nabla(\boldsymbol{u}_h^n - \boldsymbol{u}_d^n)\|_0^2 \leq \frac{1}{2}\|\boldsymbol{u}_h^n - \boldsymbol{u}_d^n - \left(\boldsymbol{u}_h^{n-1} - \boldsymbol{u}_d^{n-1}\right)\|_0^2 + \frac{1}{2}\|\boldsymbol{u}_h^n - P^d \boldsymbol{u}_h^n\|_0^2 \\
&+ Ck\|\nabla\left(\boldsymbol{u}_h^n - P^d \boldsymbol{u}_h^n\right)\|_0^2 + Ck\|p_h^n - \rho^d p_h^n\|_0^2 + C\|\bar{\partial}_t \boldsymbol{u}_h^n - \bar{\partial}_t R_d \boldsymbol{u}_h^n\|_{-1}^2 \\
&+ (\varepsilon_1 + C\varepsilon_2 + \varepsilon)k[\|\nabla(\boldsymbol{u}_h^n - \boldsymbol{u}_d^n)\|_0^2 + \|\nabla\left(\boldsymbol{u}_h^{n-1} - \boldsymbol{u}_d^{n-1}\right)\|_0^2] \\
&+ \frac{1}{2}k[N^2\gamma^{-1}\|\nabla \boldsymbol{u}_h^n\|_0^2\|\nabla(\boldsymbol{u}_h^{n-1} - \boldsymbol{u}_d^{n-1})\|_0^2 + \gamma\|\nabla(\boldsymbol{u}_h^n - \boldsymbol{u}_d^n)\|_0^2],
\end{aligned}$$

where ε_1 and ε_2 are two small positive constants which can be chosen arbitrarily. Taking $\varepsilon + \varepsilon_1 + C\varepsilon_2 = \nu/4$, it follows from (4.16) that

$$\begin{aligned}
&\left[\|\boldsymbol{u}_h^n - \boldsymbol{u}_d^n\|_0^2 - \|\boldsymbol{u}_h^{n-1} - \boldsymbol{u}_d^{n-1}\|_0^2\right] + \nu k\|\nabla(\boldsymbol{u}_h^n - \boldsymbol{u}_d^n)\|_0^2 \\
&\leq \|\boldsymbol{u}_h^n - P^d \boldsymbol{u}_h^n\|_0^2 + Ck\|\nabla(\boldsymbol{u}_h^n - P^d \boldsymbol{u}_h^n)\|_0^2 + Ck\|p_h^n - \rho^d p_h^n\|_0^2 \\
&\quad + C\|\bar{\partial}_t \boldsymbol{u}_h^n - \bar{\partial}_t R_d \boldsymbol{u}_h^n\|_{-1}^2 + \frac{1}{2}k\gamma\|\nabla\left(\boldsymbol{u}_h^{n-1} - \boldsymbol{u}_d^{n-1}\right)\|_0^2 \\
&\quad + kN^2\gamma^{-1}\|\nabla \boldsymbol{u}_h^n\|_0^2\|\nabla\left(\boldsymbol{u}_h^{n-1} - \boldsymbol{u}_d^{n-1}\right)\|_0^2, \quad 1 \leq n \leq L.
\end{aligned} \tag{4.17}$$

If $h^2 = O(k)$, $2\nu^{-2}N\sum_{j=1}^{n}\|\boldsymbol{f}^j\|_{-1} < 1$, $n = n_i$ $(i = 1, 2, \ldots, \ell)$, summing (4.17) from $n = n_1, n_2, \ldots, n_i$ $(i = 1, 2, \ldots, \ell)$, let $n_0 = 0$, and noting that $\boldsymbol{u}_h^0 - \boldsymbol{u}_d^0 = \boldsymbol{0}$ and $\ell \leq L$, from Lemmas 3.3, 4.1, and 4.2, we obtain that

$$\begin{aligned}
&\|\boldsymbol{u}_h^{n_i} - \boldsymbol{u}_d^{n_i}\|_0^2 + \nu k\|\nabla(\boldsymbol{u}_h^{n_i} - \boldsymbol{u}_d^{n_i})\|_0^2 \leq C\sum_{j=1}^{i}\|\boldsymbol{u}_h^{n_j} - P^d \boldsymbol{u}_h^{n_j}\|_0^2 \\
&+ Ck\sum_{j=1}^{i}[\|\nabla(\boldsymbol{u}_h^{n_j} - P^d \boldsymbol{u}_h^{n_j})\|_0^2 + \|p_h^{n_j} - \rho^d p_h^{n_j}\|_0^2] \\
&+ C\sum_{j=1}^{i}[\|\boldsymbol{u}_h^{n_j} - R_d \boldsymbol{u}_h^{n_j}\|_{-1}^2 + \|\boldsymbol{u}_h^{n_{j-1}} - R_d \boldsymbol{u}_h^{n_{j-1}}\|_{-1}^2] \\
&\leq Ck\sum_{j=d+1}^{l}\lambda_j, \ i = 1, 2, \ldots, \ell.
\end{aligned} \tag{4.18}$$

Thus, we obtain that

$$\begin{aligned}
&\|\boldsymbol{u}_h^{n_i} - \boldsymbol{u}_d^{n_i}\|_0 + (\nu k)^{1/2}\|\nabla(\boldsymbol{u}_h^{n_i} - \boldsymbol{u}_d^{n_i})\|_0 \\
&\le C\left(k^{1/2}\sum_{j=d+1}^{l}\lambda_j\right)^{1/2}, \ i = 1, 2, \dots, \ell.
\end{aligned} \tag{4.19}$$

Combining (4.19) and (4.14), by Lemmas 3.3, 4.1, and 4.2, we obtain the first inequality of (4.6).

If $n \neq n_i$ $(i = 1, 2, \dots, \ell)$, we may as well let $t^{(n)} \in (t^{(n_{i-1})}, t^{(n_i)})$ and $t^{(n)}$ be the nearest point to $t^{(n_i)}$. Expanding $\boldsymbol{u}^n$ and p^n into Taylor series with respect to $t^{(n_i)}$ yields that

$$\begin{aligned}
&\boldsymbol{u}^n = \boldsymbol{u}^{n_i} - \eta_i k\frac{\partial \boldsymbol{u}(\xi_1)}{\partial t}, \ t^{(n)} \le \xi_1 \le t^{(n_i)}, \\
&p^n = p^{n_i} - \eta_i k\frac{\partial p(\xi_2)}{\partial t}, \ t^{(n)} \le \xi_2 \le t^{(n_i)},
\end{aligned} \tag{4.20}$$

where η_i is the step number from $t^{(n)}$ to $t^{(n_i)}$. If $h^2 = O(k)$, $2\nu^{-2}N\sum_{j=1}^{n}\|\boldsymbol{f}^j\|_{-1} < 1$, $k = O(\ell^{-2})$, summing (4.17) for $n_1, \dots, n_{i-1}, n$, let $n_0 = 0$, and noting that $\boldsymbol{u}_h^0 - \boldsymbol{u}_d^0 = \boldsymbol{0}$, from Lemmas 4.1 and 4.2 and Lemma 3.3, we obtain that

$$\|\boldsymbol{u}_h^n - \boldsymbol{u}_d^n\|_0^2 + k\gamma\|\nabla(\boldsymbol{u}_h^n - \boldsymbol{u}_d^n)\|_0^2 \le C\eta^2k^3 + Ck^{1/2}\sum_{j=d+1}^{l}\lambda_j. \tag{4.21}$$

Since snapshots are equably taken, $\eta_i \le L/(2\ell)$. If $k = O(\ell^{-2})$, we obtain that

$$\|\boldsymbol{u}_h^n - \boldsymbol{u}_d^n\|_0 + k^{1/2}\|\nabla(\boldsymbol{u}_h^n - \boldsymbol{u}_d^n)\|_0 \le Ck + C\left(k^{1/2}\sum_{j=d+1}^{l}\lambda_j\right)^{1/2}. \tag{4.22}$$

Combining (4.22) and (4.14), by Lemmas 3.3, 4.1, and 4.2, we obtain the second inequality of (4.6). ∎

Combining Theorem 2.2 and Theorem 4.4 yields the following result.

THEOREM 4.5. *Under Theorem* 2.2 *and Theorem* 4.4 *hypotheses, the error estimate between the solutions for Problem* (II) *and the solutions for the reduced order basic Problem* (IV) *is, for* $n = 1, 2, \dots, L$, $m = 1, 2, 3$,

$$\begin{aligned}
&\|\boldsymbol{u}^n - \boldsymbol{u}_d^n\|_0 + k^{1/2}\|p^n - p_d^n\|_0 + k^{1/2}\|\nabla(\boldsymbol{u}^n - \boldsymbol{u}_d^n)\|_0 \\
&\le Ck + Ch^m + C\left(k^{1/2}\sum_{j=d+1}^{l}\lambda_j\right)^{1/2}.
\end{aligned} \tag{4.23}$$

Remark 4.6. Though the constants C in Theorems 4.4 and 4.5 are directly independent on k, they are indirectly dependent on L. Therefore, if $k \to 0$, that implies $L \to \infty$. The condition $k = O(\ell^{-2})$, which implies $L = O(\ell^2)$, in Theorem 4.4 shows the relation between the number ℓ of snapshots and the number L at all time instances. Therefore, it is unnecessary to take total transient solutions at all time instances $t^{(n)}$ as snapshots (see, for instance, in [27]–[29]). Theorems 4.4 and 4.5 have

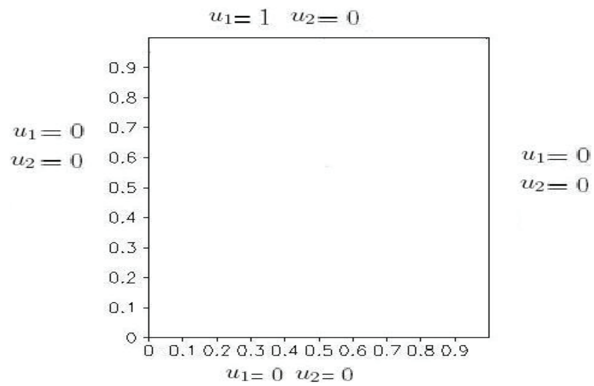

FIG. 1. *Physical model of the cavity flows: $t = 0$; i.e., $n = 0$ initial values on boundary.*

presented the error estimates between the solution of the reduced MFE formulation Problem (IV) and the solution of usual MFE formulation Problem (III) and Problem (II), respectively. Since our methods employ some MFE solutions $(\boldsymbol{u}_h^n, p_h^n)$ $(n = 1, 2, \ldots, L)$ for Problem (III) as assistant analysis, the error estimates in Theorem 4.5 are correlated to the spatial grid scale h and time step size k. However, when one computes actual problems, one may obtain the ensemble of snapshots from physical system trajectories by drawing samples from experiments and interpolation (or data assimilation). Therefore, the assistant $(\boldsymbol{u}_h^n, p_h^n)$ $(n = 1, 2, \ldots, L)$ could be replaced with the interpolation functions of experimental and previous results, thus rendering it unnecessary to solve Problem (III), and requiring only to directly solve Problem (IV) such that Theorem 4.4 is satisfied.

5. Some numerical experiments. In this section, we present some numerical examples of the physical model of cavity flows for Mini's element and different Reynolds numbers by the reduced formulation Problem (IV), thus validating the feasibility and efficiency of the POD method.

Let the side length of the cavity be 1 (see Figure 1). We first divide the cavity into $32 \times 32 = 1024$ small squares with side length $\triangle x = \triangle y = \frac{1}{32}$, and then link the diagonal of the square to divide each square into two triangles in the same direction, which consists of triangularization $\Im_h$. Take time step increment as $k = 0.001$. Except that u_1 is equal to 1 on upper boundary, all other initial value, boundary values, and (f_1, f_2) are all taken as 0 (see Figure 1).

We obtain 20 values (i.e., snapshots) at time $t = 10, 20, 30, \ldots, 200$ by solving the usual MFE formulation, i.e., Problem (III). It is shown by computing that eigenvalues satisfy $[k^{1/2} \sum_{i=7}^{20} \lambda_i]^{1/2} \leq 10^{-3}$. When $t = 200$, we obtain the solutions of the reduced formulation Problem (IV) based on the POD method of MFE depicted graphically in Figures 2 to 5 on the right-hand side employed six POD bases for $Re = 750$ and required six POD bases for $Re = 1500$, while the solutions obtained with usual MFE formulation Problem (III) are depicted graphically in Figures 2 to 5 on the left-hand side. (Since these figures are equal to solutions obtained with 20 bases, they are also referred to as the figures of the solution with full bases.)

Figure 6 shows the errors between solutions obtained with a different number of POD bases and solutions obtained with full bases. Comparing the usual MFE formulation Problem (III) with the reduced MFE formulation Problem (IV) containing six POD bases implementing 3000 times the numerical simulation computations, we

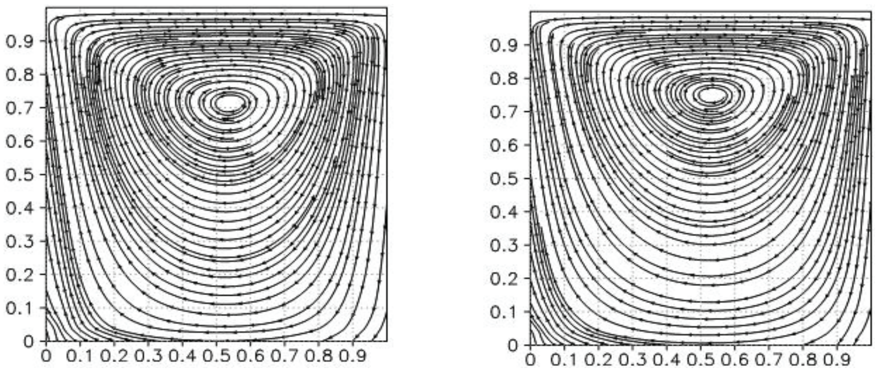

Fig. 2. *When* $Re = 750$*, velocity stream line figure for usual* MFE *solutions* (*on left-hand side figure*) *and* $d = 6$*, the solution of the reduced* MFE *formulation* (*on right-hand side figure*).

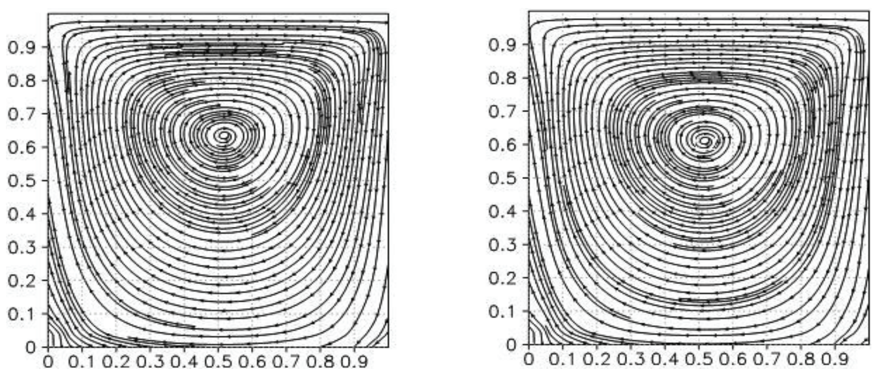

Fig. 3. *When* $Re = 1500$*, velocity stream line figure for usual* MFE *solutions* (*on left-hand side figure*) *and* $d = 6$*, the solution of the reduced* MFE *formulation* (*on right-hand side figure*).

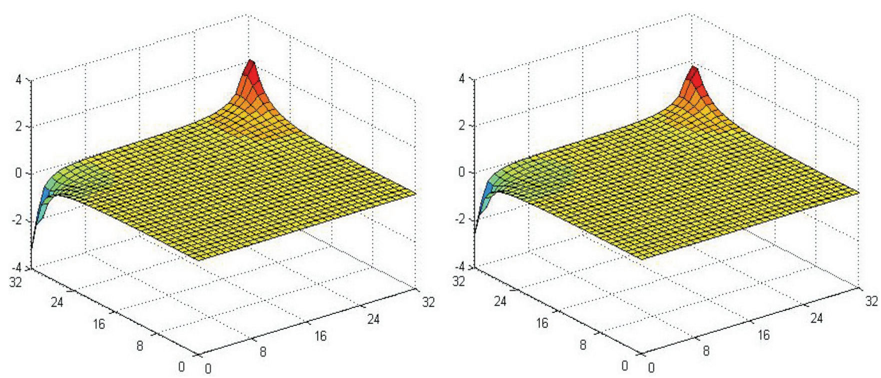

Fig. 4. *When* $Re = 750$*, pressure figure for usual* MFE *solution* (*on left-hand side figure*) *and* $d = 6$ *solution of reduced* MFE *formulation* (*on right-hand side figure*).

find that for usual MFE formulation Problem (III) the required CPU time is 6 minutes, while for the reduced MFE formulation Problem (IV) with 6 POD bases the corresponding time is only three seconds; i.e., the usual MFE formulation Problem (III) required a CPU time which is by a factor of 120 larger than that required by

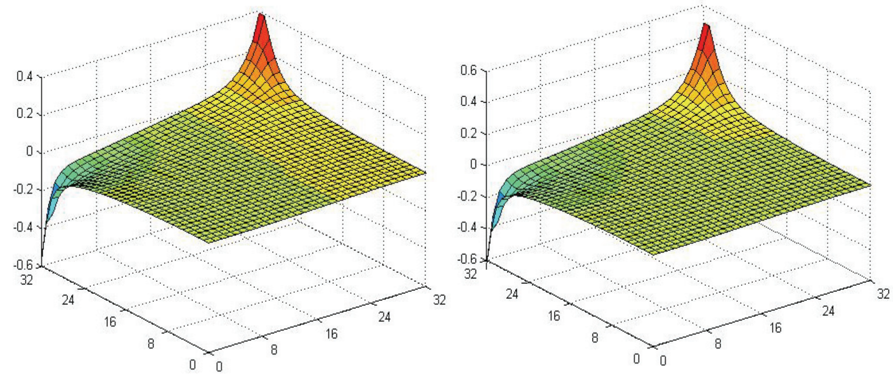

FIG. 5. *When Re* = 1500*, the pressure figure for usual* MFE *solution* (*on left-hand side figure*) *and* $d = 6$ *solution of reduced* MFE *formulation* (*on right-hand side figure*).

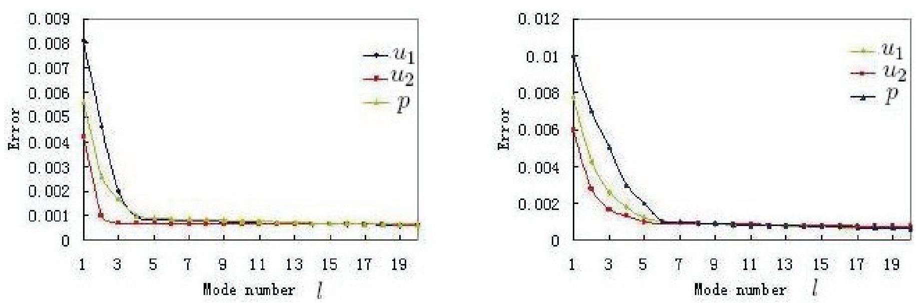

FIG. 6. *Error for Re* = 750 *on left-hand side; error for Re* = 1500 *on right-hand side.*

the reduced MFE formulation Problem (IV) with 6 POD bases, while the error between their respective solutions does not exceed 10^{-3}. It is also shown that finding the approximate solutions for the nonstationary Navier–Stokes equations with the reduced MFE formulation Problem (IV) is computationally very effective. The results for numerical examples are consistent with those obtained for the theoretical case.

6. Conclusions. In this paper, we have employed the POD technique to derive a reduced formulation for the nonstationary Navier–Stokes equations. We first reconstruct optimal orthogonal bases of ensembles of data which are compiled from transient solutions derived by using the usual MFE equation system, while in actual applications, one may obtain the ensemble of snapshots from physical system trajectories by drawing samples from experiments and interpolation (or data assimilation). For example, for weather forecast, one may use previous weather prediction results to construct the ensemble of snapshots to restructure the POD basis for the ensemble of snapshots by methods of the above section 3. We have also combined the optimal orthogonal bases with a Galerkin projection procedure, thus yielding a new reduced MFE formulation of lower dimensional order and of high accuracy for the nonstationary Navier–Stokes equations. We have then proceeded to derive error estimates between our reduced MFE approximate solutions and the usual MFE approximate solutions, and have shown, using numerical examples, that the error between the reduced MFE approximate solution and the usual MFE solution is consistent with the theoretical error results, thus validating both feasibility and efficiency of our reduced MFE formulation. Future research work in this area will aim to extend the reduced MFE formulation, applying it to a realistic operational atmospheric numerical weather forecast system and to more complicated PDEs. We have shown both by theoretical analysis as well as by numerical examples that the reduced MFE formulation presented herein has extensive potential applications.

Though Kunisch and Volkwein have presented some Galerkin proper orthogonal decomposition methods for a general equation in fluid dynamics, i.e., for the nonstationary Navier–Stokes equations in [28], our method is different from their approaches, whose methods consist of Galerkin projection approaches where the original variables are substituted for linear combination of POD basis and the error estimates of the velocity field therein are only derived, their POD basis being generated with the solutions of the physical system at all time instances, while our POD basis is generated with only few solutions of the physical system which are useful and of interest for us. Especially, only the velocity field is approximated in [28], while both the velocity field and the pressure are all synchronously approximated in our present method, and error estimates of velocity field and pressure approximate solutions are also synchronously derived. Thus, our method appears to be more optimal than that in [28].

Acknowledgments. The authors thank all referees and Professor Karl Kunisch for their valued suggestions to this paper very much.

REFERENCES

[1] V. Girault and P. A. Raviart, *Finite Element Methods for Navier–Stokes Equations, Theorem and Algorithms,* Springer-Verlag, Berlin, 1986.
[2] J. G. Heywood and R. Rannacher, *Finite element approximation of the nonstationary Navier–Stokes problem*, I. *Regularity of solutions and second order estimates for spatial discretization*, SIAM J. Numer. Anal., 19 (1982), pp. 275–311.
[3] Z. D. Luo, *The third order estimate of mixed finite element for the Navier–Stokes problems*, Chinese Quart. J. Math., 10 (1995), pp. 9–12.
[4] K. Fukunaga, *Introduction to Statistical Recognition*, Academic Press, New York, 1990.
[5] I. T. Jolliffe, *Principal Component Analysis*, Springer-Verlag, Berlin, 2002.
[6] D. T. Crommelin and A. J. Majda, *Strategies for model reduction: Comparing different optimal bases*, J. Atmospheric Sci., 61 (2004), pp. 2206–2217.
[7] A. J. Majda, I. Timofeyev, and E. Vanden-Eijnden, *Systematic strategies for stochastic mode reduction in climate*, J. Atmospheric Sci., 60 (2003), pp. 1705–1722.
[8] F. Selten, *Baroclinic empirical orthogonal functions as basis functions in an atmospheric model*, J. Atmospheric Sci., 54 (1997), pp. 2100–2114.
[9] P. Holmes, J. L. Lumley, and G. Berkooz, *Turbulence, Coherent Structures, Dynamical Systems and Symmetry*, Cambridge University Press, Cambridge, UK, 1996.
[10] G. Berkooz, P. Holmes, and J. L. Lumley, *The proper orthogonal decomposition in analysis of turbulent flows*, Ann. Rev. Fluid Mech., 25 (1993), pp. 539–575.
[11] W. Cazemier, R. W. C. P. Verstappen, and A. E. P. Veldman, *Proper orthogonal decomposition and low–dimensional models for driven cavity flows*, Phys. Fluids, 10 (1998), pp. 1685–1699.
[12] D. Ahlman, F. Södelund, J. Jackson, A. Kurdila, and W. Shyy, *Proper orthogonal decomposition for time-dependent lid-driven cavity flows*, Numerical Heal Transfer Part B–Fundamentals, 42 (2002), pp. 285–306.
[13] J. L. Lumley, *Coherent Structures in Turbulence*, in Transition and Turbulence, R. E. Meyer, ed., Academic Press, New York, 1981, pp. 215–242.
[14] Y. N. Aubry, P. Holmes, J. L. Lumley, and E. Stone, *The dynamics of coherent structures in the wall region of a turbulent boundary layer*, J. Fluid Dyn., 192 (1988), pp. 115–173.
[15] L. Sirovich, *Turbulence and the dynamics of coherent structures: Parts* I-III, Quart. Appl. Math., 45 (1987), pp. 561–590.
[16] R. D. Joslin, M. D. Gunzburger, R. A. Nicolaides, G. Erlebacher, and M. Y. Hussaini, *A self-contained automated methodology for optimal flow control validated for transition delay*, AIAA J., 35 (1997), pp. 816–824.

[17] H. V. Ly and H. T. Tran, *Proper orthogonal decomposition for flow calculations and optimal control in a horizontal CVD reactor*, Quart. Appl. Math., 60 (2002), pp. 631–656.
[18] O. K. Redionitis, J. Ko, X. Yue, and A. J. Kurdila, *Synthetic Jets, Their Reduced Order Modeling and Applications to Flow Control*, AIAA Paper number 99-1000, 37 Aerospace Sciences Meeting & Exhibit, Reno, NV, 1999.
[19] P. Moin and R. D. Moser, *Characteristic-eddy decomposition of turbulence in channel*, J. Fluid Mech., 200 (1989), pp. 417–509.
[20] M. Rajaee, S. K. F. Karlsson, and L. Sirovich, *Low dimensional description of free shear flow coherent structures and their dynamical behavior*, J. Fluid Mech., 258 (1994), pp. 1401–1402.
[21] Y. H. Cao, J. Zhu, Z. D. Luo, and I. M. Navon, *Reduced order modeling of the upper tropical pacific ocean model using proper orthogonal decomposition*, Comput. Math. Appl., 52 (2006), pp. 1373–1386.
[22] Y. H. Cao, J. Zhu, I. M. Navon, and Z. D. Luo, *A reduced order approach to four-dimensional variational data assimilation using proper orthogonal decomposition*, Internat. J. Numer. Methods Fluids, 53 (2007), pp. 1571–1583.
[23] Z. D. Luo, J. Zhu, R. W. Wang, and I. M. Navon, *Proper orthogonal decomposition approach and error estimation of mixed finite element methods for the tropical Pacific Ocean reduced gravity model*, Comput. Methods Appl. Mech. Engrg., 196 (2007), pp. 4184–4195.
[24] Z. D. Luo, J. Chen, J. Zhu, R. W. Wang, and I. M. Navon, *An optimizing reduced order FDS for the tropical Pacific Ocean reduced gravity model*, Internat. J. Numer. Methods Fluids, 55 (2007), pp. 143–161.
[25] R. W. Wang, J. Zhu, Z. D. Luo, and I. M. Navon, *An equation–free reduced order modeling approach to tropic pacific simulation*, accepted for publication in the Advances in Geosciences book series of World Scientific Publishing, 2007.
[26] Z. D. Luo, R. W. Wang, J. Chen, and J. Zhu, *Finite difference scheme based on proper orthogonal decomposition for the nonstationary Navier–Stokes equations*, Sci. China Ser. A: Math., 50 (2007), pp. 1186–1196.
[27] K. Kunisch and S. Volkwein, *Galerkin proper orthogonal decomposition methods for parabolic problems,* Numer. Math., 90 (2001), pp. 177–148.
[28] K. Kunisch and S. Volkwein, *Galerkin proper orthogonal decomposition methods for a general equation in fluid dynamics*, SIAM J. Numer. Anal., 40 (2002), pp. 492–515.
[29] K. Kunisch and S. Volkwein, *Control of Burgers' equation by a reduced order approach using proper orthogonal decomposition*, J. Optim. Theory Appl., 102 (1999), pp. 345–371.
[30] R. A. Adams, *Sobolev Space*, Academic Press, New York, 1975.
[31] P. G. Ciarlet, *The Finite Element Method for Elliptic Problems*, North-Holland, Amsterdam, 1978.
[32] F. Brezzi and M. Fortin, *Mixed and Hybrid Finite Element Methods*, Springer-Verlag, New York, 1991.
[33] Z. D. Luo, *Mixed Finite Element Methods and Applications*, Chinese Science Press, Beijing, 2006.